Analytica Chimica Acta 1233 (2022) 340519

Contents lists available at ScienceDirect

Analytica Chimica Acta

journal homepage: www.elsevier.com/locate/aca

An ultrasensitive biosensing platform for FEN1 activity detection based on target-induced primer extension to trigger the collateral cleavage of CRISPR/Cas12a

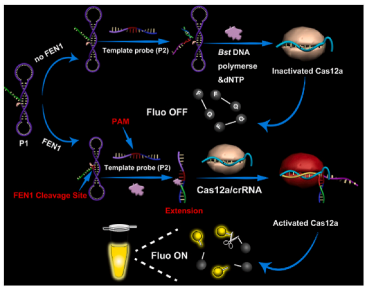
Xiaoying Cai [a,1], Dan Zhao [b,1], Xingrong Li [a], Qingyuan Zheng [a], Xiaojia Shu [a], Shijia Ding [a], Decai Zhang [c,**], Yurong Yan [a,*]

[a] Key Laboratory of Clinical Laboratory Diagnostics (Ministry of Education), College of Laboratory Medicine, Chongqing Medical University, Chongqing, 400016, China
[b] Department of Clinical Laboratory, Chongqing University Three Gorges Hospital, Chongqing, 404000, China
[c] The Center for Clinical Molecular Medical Detection, The First Affiliated Hospital of Chongqing Medical University, Chongqing, 400016, China

HIGHLIGHTS

- A CRISPR/Cas12a-driven biosensor for FEN1 activity detection was proposed.
- Target-induced DNA extension and CRISPR/Cas12a-based amplification was achieved.
- The method exhibits remarkable detection sensitivity and excellent specificity.
- The method can be employed for determinating FEN1 activity in biological samples.

GRAPHICAL ABSTRACT



ARTICLE INFO

Keywords:
Biosensor
CRISPR/Cas12a
Collateral cleavage
Fluorescence
FEN1 detection

ABSTRACT

Flap endonuclease 1 (FEN1), a structure-selective endonuclease essential for DNA replication and repair, has been considered as a new promising marker for early cancer diagnosis. However, reliable, sensitive and convenient biosensors for FEN1 detection are still technically challenging. Herein, a fluorometric biosensor based on target-induced primer extension to initiate the collateral cleavage of CRISPR/Cas12a has been established for ultrasensitive and specific detection of FEN1 activity. Using branched DNA to probe FEN1 activity, the cleaved 5′ flap initiated DNA polymerase-mediated primer extension to produce plenty of DNA duplexes containing protospacer adjacent motif (PAM) which act as activators to initiate the collateral cleavage activity of Cas12a protein, producing an significantly amplified fluorescence response for ultrasensitive determination of FEN1 activity. The developed biosensing platform displays excellent analytical performance, with a limit of detection (LOD) down to 8.9×10^{-5} U μL^{-1}, and a wide linear range from 1.0×10^{-4} to 5.0×10^{-1} U μL^{-1}. Moreover, the proposed strategy was successfully used for FEN1 detection in serums and cell lysates and suggests potential clinical applications, which may provide a reliable approach for FEN1 that will allow effective diagnosis in the early stages of related cancer.

* Corresponding author.
** Corresponding author.
E-mail addresses: zhangdecai2000@163.com (D. Zhang), yanyurong@cqmu.edu.cn (Y. Yan).
[1] These authors contributed equally to this work.

https://doi.org/10.1016/j.aca.2022.340519
Received 2 August 2022; Received in revised form 8 October 2022; Accepted 11 October 2022
Available online 14 October 2022
0003-2670/© 2022 Elsevier B.V. All rights reserved.

1. Introduction

Flap endonuclease 1 (FEN1), as a structure-selective endonuclease in eukaryotic cells, catalyzes the removal of 5′ overhanging DNA flaps from forked structures and plays a key role in DNA replication and repair because it is involved in both long-patch base excision repair (LP-BER) and Okazaki fragment maturation [1–4]. With growing evidence that the overexpression of FEN1 is related to various types of tumor onset and progression [5–7], such as ovarian carcinoma and breast cancer, FEN1 has gradually been considered as a promising diagnosis and prognosis biomarker for cancers [8,9]. Due to inhibiting FEN1 can suppress rapid tumor growth, FEN1 is also an important therapeutic target in chemotherapy [10]. Thus, monitoring FEN1 activity is of great value in clinical applications.

Unfortunately, the development of sensing approaches for determination of FEN1 activity has made limited progress. The routine methods for FEN1 measurement include immunochemistry analysis [11], western blotting [12], and enzyme-linked immunosorbent assay (ELISA) [13], which are mainly based on antigen-antibody interaction and can only be applied to qualitative and semiquantitative the FEN1 expression level. Meanwhile, these multistep and cumbersome methods suffer from detection instability, increased complexity and high cost. Recently, a few novel biosensors have been developed to overcome the drawbacks of traditional techniques. For instance, Zhang et al. designed various types of nanodevices which integrated graphene oxide (GO) nonosheets with fluorophore-labeled DNA probes for direct monitoring FEN1 activity from tumor cells [14]. Li et al. proposed a FEN1-responsive DNA-silver nanoclusters (DNA-AgNCs)-based fluorescent nanoprobe to quantify FEN1 in clinical samples [15]. Despite those progress, almost all of the reported FEN1 measurements were performed by directly reading the FEN1 enzymatic activity, which leads to limited sensitivity. Therefore, convenient and ultrasensitive biosensing techniques for detecting FEN1 activity are urgently needed.

Clustered regularly interspaced short palindromic repeats (CRISPR) and CRISPR-associated (Cas) system is an adaptive immune mechanism in prokaryotes, it can bind to a programmable guide RNA (gRNA) that directs Cas effectors to cleave foreign nucleic acids [16–19]. Due to the excellent recognition specificity and cutting features, CRISPR-Cas system has emerged as one of the most powerful toolboxes in the field of molecular biology, especially in gene-editing [20–22]. Additionally, some recently discovered Cas proteins possess collateral cleavage (*trans*-cleavage) capabilities, such as Cas12a, Cas13a and *etc*. [23–25], making them a hot spot in biosensing fields because they can address recognition, transduction and amplification elements in one system. The CRISPR-based biosensors have some obvious advantages, including mild reaction temperature, easy operation, excellent specificity and high signal amplification efficiency [26–28]. In the case of nucleic acid sensing, the experimental process typically entails (i) the pre-amplification of target nucleic acid, (ii) the identification of the amplified products containing protospacer adjacent motif (PAM), and (iii) the collateral cleavage of nontargeted nucleic acid reporters containing fluorophore-quencher pairs. The cutting of the reporters causes the fluorophore to be released from the quencher, producing amplified fluorescence signals. The CRISPR-based biosensors can also be used to detect proteins [29,30], small molecules [31], and enzyme activities [32,33] through the introduction of functional nucleic acids that convert non-nucleic acid targets into nucleic acid intermediates. As FEN1 cleaves branched structures of DNA intermediates rather than specific DNA sequences and forms DNA fragments containing 3′-OH terminal, the cleaved fragments can bind to template strands that are flexibly defined by users and can be used as primers to synthesize duplex DNA products for various purposes with the participation of DNA polymerases [34]. This feature can be seamlessly integrated with CRISPR systems, particularly CRISPR/Cas12a, which is activated by double-stranded DNA containing PAM sites [24], for the development of biosensing platforms. To the best of our knowledge, however, there is no existing sensing method based on CRISPR that allows direct and convenient detection of FEN1 enzymatic activity.

Herein, we present the development and demonstration of a fluorometric biosensor based on target-induced primer extension to initiate the collateral cleavage of CRISPR/Cas12a for ultrasensitive FEN1 determination. We employed FEN1 branching enzymatic activity and *Bst* DNA polymerase-assisted primer extension to generate numerous double strand DNA (dsDNA) activators that initiate Cas12a collateral cleavage effect to develop an efficient signal amplification system with highly modular design. According to the multi-turnover collateral cleavage of activated Cas12a, efficient amplification and rapid response periods can be easily obtained. Under the optimal conditions, this approach can detect FEN1 activity from 1.0×10^{-4} to 5.0×10^{-1} U μL^{-1} with detection limits down to 8.9×10^{-5} U μL^{-1}, which is much lower than that of most existing assays. And the serum interference test and the examination of FEN1 activity in diluted serum samples and cell lysates demonstrated that the biosensing method could be applied to analyze FEN1 activity in real samples.

2. Materials and methods

2.1. FEN1 detection procedure

Briefly, 1 μL of 1.5 μM P1 and 5 μL of FEN1 with different concentrations were incubated in buffer solution (20 μL) containing 1 × Thermo Pol Reaction Buffer (0.01 M KCl, 0.02 M Tris-HCl, 0.01 M $(NH4)_2SO_4$, 0.002 M $MgSO_4$, 0.1% Triton X-100, pH 8.9) at 37 °C for 0.5 h. Subsequently, 1 μL of 400 nM P2, 1 μL of 0.3 U μL^{-1} *Bst* polymerase, and 1 μL of 2 mM dNTPs were mixed with 3 μL of 10 × NEBuffer 3 (1 M NaCl, 0.5 M Tris-HCl, 0.1 M $MgCl_2$, 0.01 M DTT, pH 7.9) in total volume of 30 μL, then the mixture was placed at 55 °C for 0.5 h. Afterward, the Cas12a cleavage reaction was performed by mixing a reaction solution containing 50 nM Cas12a/crRNA complex (Cas12a: crRNA = 1 : 1), 40 U RNase inhibitor, and 500 nM FQ-ssDNA. After reaction at 37 °C for 1 h, the fluorescent spectrum was detected using a Cary Eclipse fluorescence spectrophotometer with excitation and emission at 492 nm and 520 nm, respectively.

2.2. Detection of FEN1 in cancer cells

The SMMC-7721 and glioma U87 cell lines were cultured in DMEM medium containing 10% FBS and 1% penicillin/streptomycin in 5% CO_2 in humidified air at 37 °C. The cell lysates were obtained by RIPA Lysis Buffer. The collected lysates were divided and stored at −80 °C until utilization. FEN1 activity detection in cell lysates were performed according to the above mentioned procedures.

2.3. Enzyme-linked immunosorbent assays

FEN1 levels were measured in SMMC-7721 and glioma U87 cells using enzyme-linked immunosorbent assay (ELISA) (kit from Fine Biotech, Wuhan, China) according to the manufacturer's protocol. Briefly, cells were separated by trypsin, washed with PBS, and resuspended in fresh lysis buffers. Cell debris were removed by centrifugation at 12,000 rpm for 30 min at 4 °C. The obtained cell lysates were added into a 96-well strip plate pre-coated with FEN1 antibodies for ELISA analysis. Measurements were carried out using a spectrophotometer (Thermo Scientific, USA) at the wavelength of 450 nm.

2.4. Polyacrylamide gel electrophoresis (PAGE) assay

A 12% native PAGE was prepared to evaluate the FEN1 cleavage, the extension reaction, and the collateral cleavage effect of Cas12a. Electrophoresis was carried out in 1 × TBE buffer (2 mM EDTA, 90 mM Tris-borate, pH 8.4) at 110 V for 50 min at room temperature. Afterward, the gel was immersed in a freshly prepared stain-all solution (containing 4

μL of GoldView in 80 mL of 1 × TBE) for 35 min. Subsequently, the PAGE results were scanned by a gel image analysis platform.

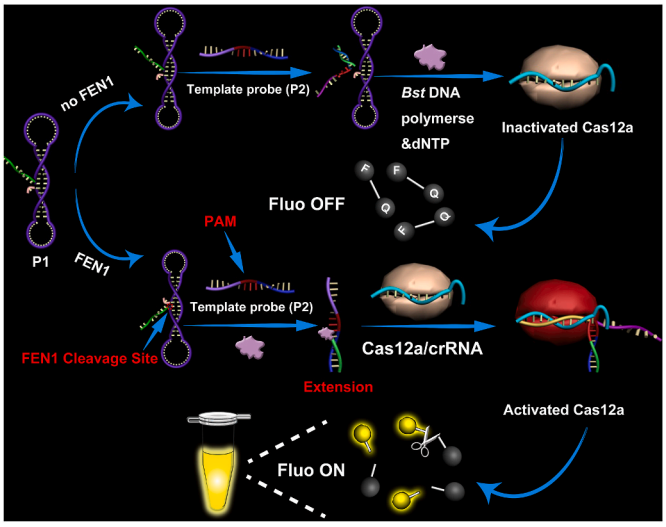
3. Results and discussion

3.1. Design of the fluorometric biosensor

Previous studies have shown that CRISPR/Cas12a can cleave double-stranded DNA under the guidance of CRISPR RNA (crRNA), and release collateral cleavage activity with extremely high turnover rate (~1250 turnovers per second) [35]. In this study, CRISPR/Cas12a was served as a signal amplifier for FEN1 activity determination. The working mechanism of the sensing strategy is shown in Scheme 1. Based on previous reports, the most efficient cleavage of 5′ flap was subjected to ordered helical arch of FEN1, which would undergo disorder-to-order transition when the 3′ flap binding pocket of FEN1 bound to the substrate containing 1 nt 3′ flap [36,37]. Thus, a branched double-stranded DNA probe (P1) with a 5′ flap and 1 nt 3′ tail was designed for FEN1 cleavage. To avoid the need for annealing of multiple DNA strands, dumbbell-shaped P1 was prepared by single-strand DNA self-folding. In the presence of FEN1, the 5′ overhanging flap in the branched P1 would be excised. Subsequently, the released 5′ flap containing 3′-OH terminal was annealed with template probe (P2) at binding site domain (blue) and acted as primer to initiate the extension process. Under the participation of DNA polymerase, dNTPs could be gradually polymerized at the 3′-end of the primer and extended along P2 to synthesize the DNA duplex. Thus, amounts of double-stranded DNA containing PAM site (red) and crRNA-binding region (yellow) were produced, which could be recognized by Cas12a/crRNA complex and serve as activators to unlock the collateral cleavage capability of Cas12a protein. Therefore, the activated CRISPR/Cas12a can indiscriminately cut the 5′-fluorophore (FAM) and 3′-quencher (BHQ1)-labeled single-stranded DNA reporters (FQ-ssDNA) and finally produce an significantly amplified fluorescence signal. In the absence of FEN1, the P1 remains intact and *Bst* DNA polymerase-assisted primer extension cannot be triggered. Thus, the collateral cleavage capability of Cas12a is inhibited and fluorescence enhancement cannot be observed.

3.2. Feasibility analysis of the developed biosensor

To verify the design of the sensing strategy, a fluorescent scan was first conducted, and the results are provided in Fig. 1A. It can be found



Scheme 1. Schematic for the working mechanism of the fluorometric biosensor based on target-induced primer extension and the collateral cleavage of CRISPR/Cas12a.

that the FQ-ssDNA as Cas12a collateral cleavage substrates were efficiently cleaved under the assistance of *Bst* DNA polymerase and produced a robust fluorescence output (red line) when FEN1 was introduced. In contrast, the blank control without FEN1 showed only a minimal fluorescence signal (cyan line). In the absence of P1, P2, *Bst* DNA polymerase or Cas12a/crRNA complex, the fluorescence intensity was comparable to the blank control (blue, yellow, magenta and green line). Under 254 nm ultraviolet light, the fluorescence can be observed by naked eyes (Fig. 1A, inset). These results suggested that the collateral cleavage capability of Cas12a could be effectively activated in the presence of FEN1. To further validate the entire process step by step, gel electrophoresis was further performed. As depicted in Fig. 1B, P1 (lane 1) and P2 (lane 2) represented distinct bands, respectively. Lane 3 showed the combination production of P1 and P2 owing to 20 bases complementing each other. Lane 6 contained the bands among which the lowest band demonstrated that P1 was cleaved by FEN1. After mixing P2 and *Bst* DNA polymerase, the extended products presented slower migrated band than P2, implying successful synthesis of the double-stranded DNA product in the presence of DNA polymerase (lane 7). In contrast, in the absence of FEN1, double-stranded DNA product cannot be produced (lane 8). Additional ssDNA (26 nt) represented single band (lane 4). With the addition of the Cas12a/crRNA, ssDNA was *trans*-cleaved by Cas12a (lane 9). Without FEN1, Cas12a cannot be activated due to no double-stranded DNA activator production, and ssDNA remains in its original position (lane 10). All of the results suggested that the developed biosensor could be well used for FEN1 detection.

3.3. Optimization of experimental parameters

Several critical experimental parameters, consisting of the concentration of P1, P2, polymerase, and Cas12a/crRNA complex were evaluated to achieve optimal analytical performance for FEN1 detection. First, the influence of P1 concentrations from 0.5 to 2.5 μM for FEN1 cleavage were evaluated. As depicted in Fig. 2A, the signal-to-background (S/B) ratio improved with the increase of P1 concentration until the concentration reaches 1.5 μM, indicating that 1.5 μM was the optimal concentration. Then the effect of the concentration of P2 and *Bst* DNA polymerase on the extension process were studied. As depicted in Fig. 2B, with the increasing of P2 from 0.1 to 1.3 μM, the S/B formed an upward trend from 0.1 to 0.4 μM. After that, the trend was declined. Thus, 0.4 μM P2 was chosen in the following experiment. Furthermore, with the increasing of the concentration of *Bst* DNA polymerase, the S/B gradually increased before 0.3 U μL^{-1}, then reached the platform. Therefore, we selected 0.3 U μL^{-1} *Bst* DNA polymerase as the optimized concentration (Fig. 2C). The concentration of Cas12a/crRNA complex is an essential factor influencing the efficiency of Cas12a-mediated cutting reaction. Thus, the effect of the concentrations of Cas12a/crRNA complex from 0.1 to 10 μM are finally assessed, and the data is shown in Fig. 2D. For different concentrations of Cas12a/crRNA complex, the S/B ratio achieved the maximum at 5 μM. Therefore, we selected 5 μM Cas12a/crRNA complex in subsequent experiments.

3.4. Analytical performance

Under the optimized experimental parameters, the linear range and detection limit of the constructed biosensor were evaluated toward FEN1 at various concentrations. As shown in Fig. 3A, the fluorescent intensity increased with increasing FEN1 concentration. According to the calibration plot of the fluorescent intensity versus the logarithm of FEN1 concentration in Fig. 3B, a linear regression equation is $Y = 254.87 \lg C + 1070.87$ (where Y stands for fluorescent intensity and C strands for the concentration of target FEN1) in a dynamic range from 1.0×10^{-4} U μL^{-1} to 5.0×10^{-1} U μL^{-1} with the correlation coefficients (R)-square of 0.995. The limit of quantification (LOQ) is 1.0×10^{-4} U μL^{-1} (~240.6 fM), and the limit of detection (LOD) is estimated to be

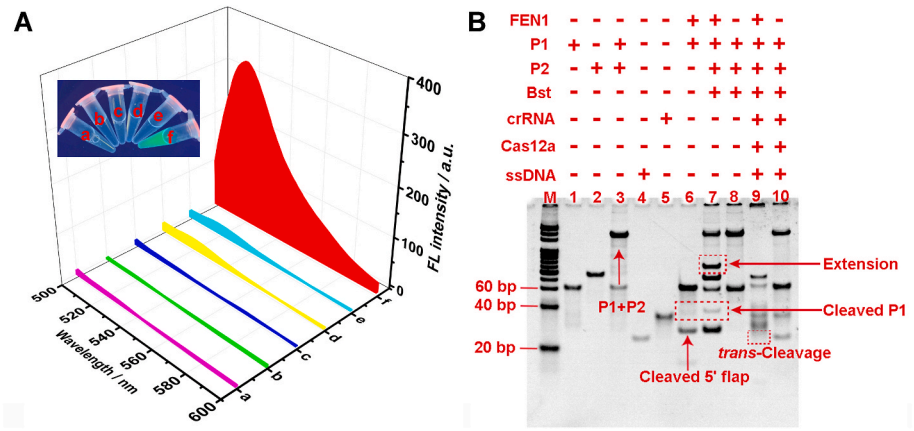


Fig. 1. (A) Fluorescence spectra of different sensing systems: (a) without Bst DNA polymerase; (b) without Cas12a/crRNA; (c) without P1; (d) without P2; (e) without FEN1; (f) with all. Inset: fluorescence image photographed with a smartphone under 254 nm ultraviolet light. (B) PAGE analysis of the products under different conditions. Lane 1: P1; lane 2: P2; lanes 3: P1 + P2; lane 4: ssDNA; lane 5: crRNA; lane 6: FEN1 + P1; lane 7: FEN1 + P1 + P2 + *Bst* DNA polymerase; lane 8: P1 + P2 + *Bst* DNA polymerase; lane 9: FEN1 + P1 + P2 + *Bst* DNA polymerase + Cas12a/crRNA complex + ssDNA; lane 10: P1 + P2 + *Bst* DNA polymerase + Cas12a/crRNA complex + ssDNA.

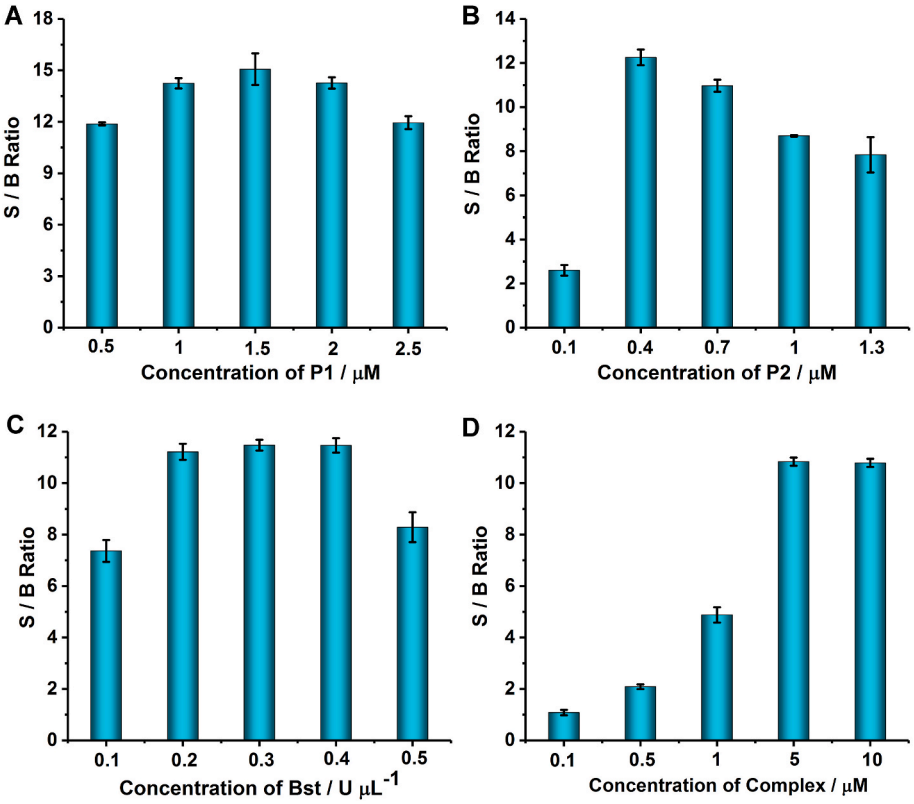


Fig. 2. Condition optimization of the FEN1 assay. Effect of (A) the concentration of P1(with 0.5 μM P2, 0.4 U μL^{-1} Bst, 5 μM Cas12a/crRNA, and 0.5 U μL^{-1} FEN1), (B) the concentration of P2 (with 1.5 μM P1, 0.4 U μL^{-1} Bst, 5 μM Cas12a/crRNA, and 0.1 U μL^{-1} FEN1), (C) the concentration of Bst DNA polymerase (with 1.5 μM P1, 0.4 μM P2, 5 μM Cas12a/crRNA, and 0.1 U μL^{-1} FEN1), and (D) the concentration of Cas12a/crRNA complex 1(with 1.5 μM P1, 0.4 μM P2, 0.3 U μL^{-1} Bst, and 0.1 U μL^{-1} FEN1). Error bars were from three repetitive measurements (λ_{ex}: 492 nm,λ_{em}: 520 nm).

8.9×10^{-5} U μL^{-1} (~214.6 fM) based on the mean of the blank plus three times of the standard deviation (3σ rule). Such detection limits for monitoring of FEN1 activity are comparable or even superior to most existing methods for FEN1 detection (Table S2).

Moreover, the selectivity of the biosensor was investigated by using some other important protein enzymes (*i.e.* FspI, MboI, UDG, DpnI, KF, and APE1). As shown in Fig. 3C and D, compared with the FEN1, the other six interference exhibit a low fluorescence intensity even though their amounts were 10 times higher than that of FEN1, indicating the excellent selectivity of this biosensor. Moreover, to evaluate the reproducibility of the biosensor, six parallel tests have been conducted for 1.0×10^{-3} U μL^{-1} target FEN1. An excellent reproducibility has been observed with low relative standard deviation (RSD <5%) (Fig. S1).

3.5. Detection of FEN1 in biological samples

Given the good analytical performance of the proposed biosensor, its applicability and specificity for detecting FEN1 target in biological samples were investigated. The matrix effect of the method was tested by spiking FEN1 in serially diluted (100-fold, 50-fold, 20-fold, 10-fold, 5-fold, 2-fold, 1-fold) serum samples via standard addition procedure. It was observed that the serum only has a slight matrix effect on the biosensor even 10-fold diluted serum samples (Table S3, Fig. 4A and B). The recoveries of the samples ranged from 94.9% to 106.7% and the RSDs were all less than 6.6% (Table S4). To further investigate the application potential of this biosensor, the fluorescent experiments were carried out in several different cell types. Results in Fig. 4C revealed that the sustained upregulation of FEN1 has been observed in SMMC-7721 and glioma U87 cell lysates, which is consistent with the result determined by commercially available kits. These results suggested that the

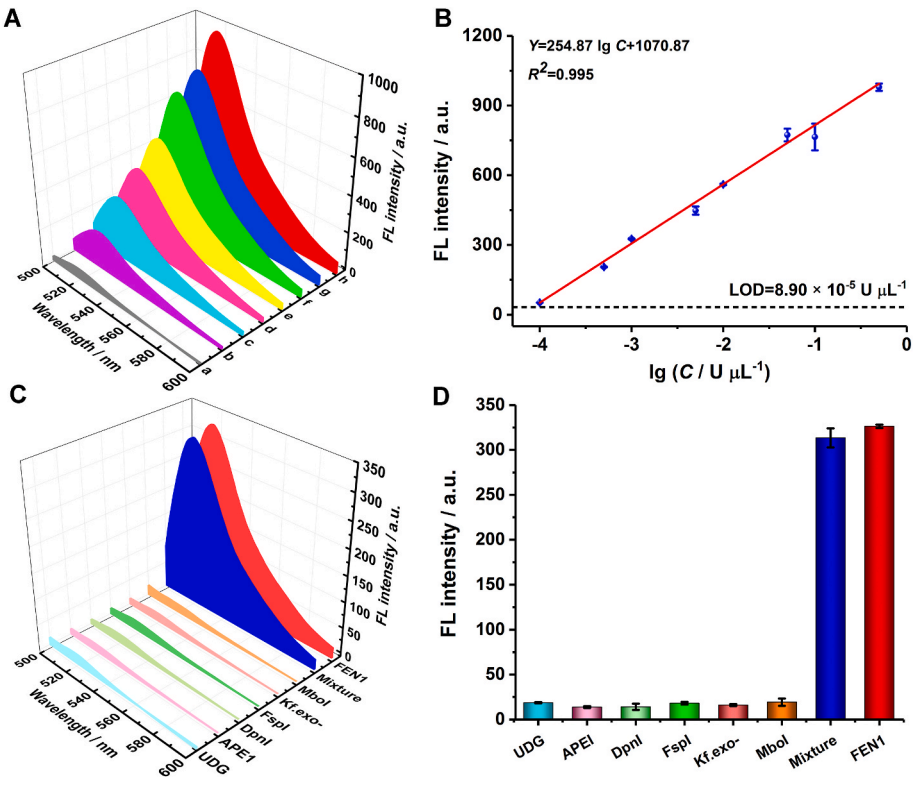


Fig. 3. Investigation of the sensitivity and selectivity of the developed sensing strategy. (A) Fluorescence spectra of various FEN1 concentrations (from a to h: 1.0×10^{-4}, 5.0×10^{-4}, 1.0×10^{-3}, 5.0×10^{-3}, 1.0×10^{-2}, 5.0×10^{-2}, 1.0×10^{-1}, 5.0×10^{-1} U μL^{-1}). (B) Linear relationship between fluorescent intensity and the logarithm concentration of FEN1. (C) and (D) shown the fluorescence spectra and corresponding fluorescence intensity of the system towards 1.0×10^{-3} U μL^{-1} of FEN1, 1.0×10^{-2} U μL^{-1} of FspI, MboI, UDG, DpnI, KF, APE1 and their mixture. Error bars were from three repetitive measurements.

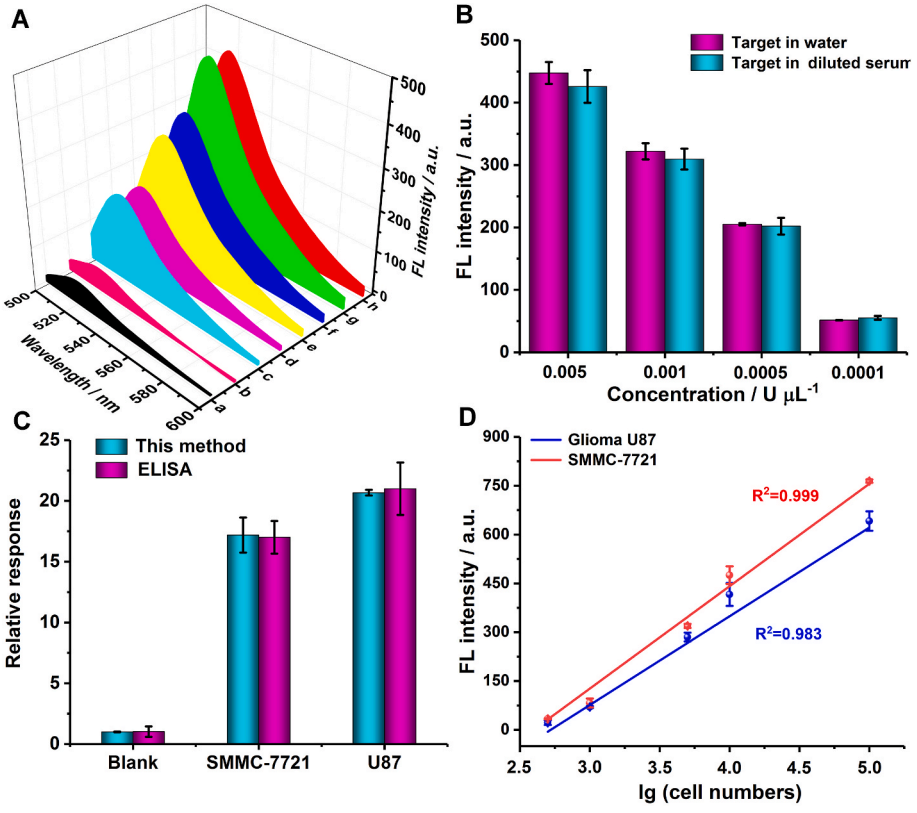


Fig. 4. (A) Fluorescence spectra of different concentrations of FEN1 added into water and 10-fold diluted healthy human serum:
(a) 1.0×10^{-4} U μL^{-1} FEN1 in diluted serum; (b) 1.0×10^{-4} U μL^{-1} FEN1 in water; (c) 5.0×10^{-4} U μL^{-1} FEN1 in diluted serum; (d) 5.0×10^{-4} U μL^{-1} FEN1 in water; (e) 1.0×10^{-3} U μL^{-1} FEN1 in diluted serum; (f) 1.0×10^{-3} U μL^{-1} FEN1 in water; (g) 5.0×10^{-3} U μL^{-1} FEN1 in diluted serum; (h) 5.0×10^{-3} U μL^{-1} FEN1 in water. (B) Comparison of fluorescence intensities between diluted serum and water. (C) FEN1 quantification in SMMC-7721 cells (5×10^4 cells) and glioma U87 cells (5×10^5 cells) using the developed biosensor and commercial ELISA kits. (D) The linear relationship between the fluorescent intensity and the logarithm cell number of SMMC-7721 and glioma U87 cells. Error bars were from three repetitive measurements.

method has potential for specific detection of FEN1 in real samples. In addition, extremely low fluorescence signal was obtained after the cell lysates pretreated with ATA and FEN1-IN-3, and there was little effect on fluorescence signal when cell lysates were pretreated with Curcumin (Fig. S2), indicating that the fluorescent response was indeed induced by active FEN1 in cells. As depicted in Fig. 4D, a good linear correlation between the fluorescence intensity and the logarithm value of cell numbers was obtained for both SMMC-7721 and glioma U87 cells from

5×10^2 to 1×10^5 cells. The above mentioned results indicated that the biosensing method can be used for screening FEN1 inhibitors and quantitative detecting FEN1 activity in tumor cells, suggesting the great potential in biomedical research and precision medicine applications.

4. Conclusion

In summary, a new fluorometric biosensor has been successfully established for ultrasensitive and selective detection of FEN1 activity by integrating target-induced primer extension with the collateral cleavage of CRISPR/Cas12a. Compared to current methods, the proposed biosensor possesses its own remarkable advantages. First, owing to the synergistic effect of enzymes, including the site-specific cleavage of branched DNA by target FEN1, sequence-dependent DNA polymerase extension, and efficient signal amplification provided by collateral cleavage capability of activated Cas12a, the established strategy exhibits remarkable detection sensitivity (LOD, 8.9×10^{-5} U μL^{-1}) and good selectivity as well as a wide dynamic range (from 1.0×10^{-4} to 5.0×10^{-1} U μL^{-1}). Second, compared with the immunological methods, targeting enzyme activity in our method is of more significant to assess the intracellular expression and activity status of FEN1. Third, the mild experimental conditions greatly reduce the special requirement for the complicated instruments and make the operation process more convenient. Moreover, this sensing method was demonstrated to work well for FEN1 detection in diluted serums and cell lysates and exhibited great potential for inhibitor screening. However, our method can be further integrated with portable fluorescence spectrophotometer to improve its detection ability in the field. The compatibility of the proteases will be studied in the future, thus combining the processing steps and shortening the reaction time. Overall, we expect that the proposed strategy would provide a convenient, inexpensive and robust biosensing platform for FEN1 activity analysis in biomedical research and precision medicine practice.

CRediT authorship contribution statement

Xiaoying Cai: Conceptualization, Methodology, Software, Investigation, Data curation, Writing – original draft. **Dan Zhao:** Methodology, Writing – review & editing. **Xingrong Li:** Methodology, Formal analysis, Software. **Qingyuan Zheng:** Methodology, Formal analysis. **Xiaojia Shu:** Software, Data curation, Software, Data curation. **Shijia Ding:** Conceptualization, Resources. **Decai Zhang:** Resources, Validation, Data curation, Writing – review & editing. **Yurong Yan:** Supervision, Methodology, Funding acquisition, Project administration, Data curation.

Declaration of competing interest

The authors declare that they have no known competing financial interests or personal relationships that could have appeared to influence the work reported in this paper.

Data availability

Data will be made available on request.

Acknowledgments

This work was supported by the National Natural Science Foundation of China (81371904, 82102505), the National Science and Technology Major Project of the Ministry of Science and Technology of China (2018ZX10732202) and the Chongqing Postgraduate Research Innovation Project (CYS21231).

Appendix A. Supplementary data

Supplementary data to this article can be found online at https://doi.org/10.1016/j.aca.2022.340519.

References

[1] S.I. Algasaier, L.D. Finger, I.A. Bennet, J.A. Grasby, Flap endonuclease 1 mutations A159V and E160D cause genomic instability by slowing reaction on double-flap substrates, Biochemistry 57 (2018) 6838–6847.
[2] J.C. Exell, M.J. Thompson, L.D. Finger, S.J. Shaw, J. Debreczeni, T.A. Ward, C. McWhirter, C.L. Sioberg, D. Martinez Molina, W.M. Abbott, C.D. Jones, J. W. Nissink, S.T. Durant, J.A. Grasby, Cellular active N-hydroxyurea FEN1 inhibitors block substrate entry to the active site, Nat. Chem. Biol. 12 (2016) 815–821.
[3] L. He, L. Luo, H. Zhu, H. Yang, Y. Zhang, H. Wu, H. Sun, F. Jiang, C.S. Kathera, L. Liu, Z. Zhuang, H. Chen, F. Pan, Z. Hu, J. Zhang, Z. Guo, FEN1 promotes tumor progression and confers cisplatin resistance in non-small-cell lung cancer, Mol. Oncol. 11 (2017) 640–654.
[4] K.A. Mesquita, R. Ali, R. Doherty, M.S. Toss, I. Miligy, A. Alblihy, D. Dorjsuren, A. Simeonov, A. Jadhav, D.M. Wilson III, I. Hickson, N.J. Tatum, E.A. Rakha, S. Madhusudan, FEN1 blockade for platinum chemo-sensitization and synthetic lethality in epithelial ovarian cancers, Cancers 13 (2021) 1866.
[5] T.M. Abdel-Fatah, R. Russell, N. Albarakati, D.J. Maloney, D. Dorjsuren, O. M. Rueda, P. Moseley, V. Mohan, H. Sun, R. Abbotts, A. Mukherjee, D. Agarwal, J. L. Illuzzi, A. Jadhav, A. Simeonov, G. Ball, S. Chan, C. Caldas, I.O. Ellis, D. M. Wilson III, S. Madhusudan, Genomic and protein expression analysis reveals flap endonuclease 1 (FEN1) as a key biomarker in breast and ovarian cancer, Mol. Oncol. 8 (2014) 1326–1338.
[6] A. Al-Kawaz, I.M. Miligy, M.S. Toss, O.J. Mohammed, A.R. Green, S. Madhusudan, E.A. Rakha, The prognostic significance of flap endonuclease 1 (FEN1) in breast ductal carcinoma in situ, Breast Cancer Res. Treat. 188 (2021) 53–63.
[7] C. Li, D. Zhou, H. Hong, S. Yang, L. Zhang, S. Li, P. Hu, H. Ren, Z. Mei, H. Tang, TGFβ1-miR-140-5p axis mediated up-regulation of flap endonuclease 1 promotes epithelial-mesenchymal transition in hepatocellular carcinoma, Aging 11 (2019) 5593–5612.
[8] L. Balakrishnan, R.A. Bambara, Flap endonuclease 1, Annu. Rev. Biochem. 82 (2013) 119–138.
[9] B. Zhou, L. Lin, B. Li, Exponential amplification reaction-based fluorescent sensor for the sensitive detection of tumor biomarker flap endonuclease 1, Sensor. Actuator. B Chem. 346 (2021), 130457.
[10] J.L. Li, J.P. Wang, H. Chang, S.M. Deng, J.H. Du, X.X. Wang, H.J. Hu, D.Y. Li, X. B. Xu, W.Q. Guo, Y.H. Song, Z. Guo, M.X. Sun, Y.W. Wu, S.B. Liu, FEN1 inhibitor increases sensitivity of radiotherapy in cervical cancer cells, Cancer Med. 8 (2019) 7774–7780.
[11] K. Zhang, S. Keymeulen, R. Nelson, T.R. Tong, Y.C. Yuan, X. Yun, Z.J. Liu, Lopez, D. J. Raz, J.Y. Kim, Overexpression of flap endonuclease 1 correlates with enhanced proliferation and poor prognosis of non-small-cell lung cancer, Am. J. Pathol. 188 (2018) 242–251.
[12] L. Ma, X. Cao, H. Wang, K. Lu, Y. Wang, C. Tu, Y. Dai, Y. Meng, Y. Li, P. Yu, S. Man, A. Diao, Discovery of myricetin as a potent inhibitor of human flap endonuclease 1, which potentially can be used as sensitizing agent against HT-29 human colon cancer cells, J. Agric. Food Chem. 67 (2019) 1656–1665.
[13] L. He, Y. Zhang, H. Sun, F. Jiang, H. Yang, H. Wu, T. Zhou, S. Hu, C.S. Kathera, X. Wang, H. Chen, H. Li, B. Shen, Y. Zhu, Z. Guo, FEN1 promotes tumor progression and confers cisplatin resistance in non-small cell lung cancer, EBioMedicine 14 (2016) 32–43.
[14] H. Zhang, S. Ba, D. Mahajan, J.Y. Lee, R. Ye, F. Shao, L. Lu, T. Li, Versatile types of DNA-based nanobiosensors for specific detection of cancer biomarker FEN1 in living cells and cell-free systems, Nano Lett. 18 (2018) 7383–7388.
[15] B. Li, P. Zhang, B. Zhou, S. Xie, A. Xia, T. Suo, S. Feng, X. Zhang, Fluorometric detection of cancer marker FEN1 based on double flapped dumbbell DNA nanoprobe functionalized with silver, Anal. Chim. Acta 1148 (2021), 238194.
[16] M.M. Kaminski, O.O. Abudayyeh, J.S. Gootenberg, F. Zhang, J.J. Collins, CRISPR-based diagnostics, Nat. Biomed. Eng. 5 (2021) 643–656.
[17] S.Y. Li, Q.X. Cheng, J.K. Liu, X.Q. Nie, G.P. Zhao, J. Wang, CRISPR-Cas12a has both cis- and trans-cleavage activities on single-stranded DNA, Cell Res. 28 (2018) 491–493.
[18] L. Oesinghaus, F.C. Simmel, Switching the activity of Cas12a using guide RNA strand displacement circuits, Nat. Commun. 10 (2019) 2092.
[19] T. Tian, Z. Qiu, Y. Jiang, D. Zhu, X. Zhou, Exploiting the orthogonal CRISPR-Cas12a/Cas13a trans-cleavage for dual-gene virus detection using a handheld device, Biosens. Bioelectron. 196 (2021), 113701.
[20] K. Krumbach, C.K. Sonntag, L. Eggeling, J. Marienhagen, CRISPR/Cas12a mediated genome editing to introduce amino acid substitutions into the mechanosensitive channel mscCG of corynebacterium glutamicum, ACS Synth. Biol. 8 (2019) 2726–2734.
[21] M.Y. Yan, H.Q. Yan, G.X. Ren, J.P. Zhao, X.P. Guo, Y.C. Sun, CRISPR-Cas12a-assisted recombineering in bacteria, Appl. Environ. Microbiol. 83 (2017), e00947.
[22] R. Zhao, Y. Liu, H. Zhang, C. Chai, J. Wang, W. Jiang, Y. Gu, CRISPR-Cas12a-mediated gene deletion and regulation in *clostridium ljungdahlii* and its application in carbon flux redirection in synthesis gas fermentation, ACS Synth. Biol. 8 (2019) 2270–2279.

[23] O.O. Abudayyeh, J.S. Gootenberg, S. Konermann, J. Joung, I.M. Slaymaker, D. B. Cox, S. Shmakov, K.S. Makarova, E. Semenova, L. Minakhin, K. Severinov, A. Regev, E.S. Lander, E.V. Koonin, F. Zhang, C2c2 is a single-component programmable RNA-guided RNA-targeting CRISPR effector, Science 353 (2016) aaf5573.
[24] J. Chen, E. Ma, L. Harrington, C.M. Da, X. Tian, J. Palefsky, J. Doudna, CRISPR-Cas12a target binding unleashes indiscriminate single-stranded DNase activity, Science 360 (2018) 436–439.
[25] L. Harrington, D. Burstein, J.S. Chen, D. Paez-Espino, E. Ma, I.P. Witte, J.C. Cofsky, N.C. Kyrpides, J.F. Banfield, J.A. Doudna, Programmed DNA destruction by miniature CRISPR-Cas14 enzymes, Science 362 (2018) 839–842.
[26] X. Li, D. Zhang, X. Gan, P. Liu, Q. Zheng, T. Yang, G. Tian, S. Ding, Y. Yan, A cascade signal amplification based on dynamic DNA nanodevices and CRISPR/Cas12a trans-cleavage for highly sensitive microRNA sensing, ACS Synth. Biol. 10 (2021) 1481–1489.
[27] B. Pang, J. Xu, Y. Liu, H. Peng, W. Feng, Y. Cao, J. Wu, H. Xiao, K. Pabbaraju, G. Tipples, M.A. Joyce, H.A. Saffran, D.L. Tyrrell, H. Zhang, X.C. Le, Isothermal amplification and ambient visualization in a single tube for the detection of SARS-CoV-2 using loop-mediated amplification and CRISPR technology, Anal. Chem. 92 (2020) 16204–16212.
[28] R. Zhou, Y. Li, T. Dong, Y. Tang, F. Li, A sequence-specific plasmonic loop-mediated isothermal amplification (LAMP) assay with orthogonal color readouts enabled by CRISPR Cas12a, Chem. Commun. 56 (2020) 3536–3538.
[29] B. Li, A. Xia, S. Zhang, T. Suo, Y. Ma, H. Huang, X. Zhang, Y. Chen, X. Zhou, A CRISPR-derived biosensor for the sensitive detection of transcription factors based on the target-induced inhibition of Cas12a activation, Biosens. Bioelectron. 173 (2020), 112619.
[30] Y. Li, H. Mansour, C.J.F. Watson, Y. Tang, A.J. MacNeil, F. Li, Amplified detection of nucleic acids and proteins using an isothermal proximity CRISPR Cas12a assay, Chem. Sci. 12 (2021) 2133–2137.
[31] W. Feng, A.M. Newbigging, J. Tao, Y. Cao, H. Peng, C. Le, J. Wu, B. Pang, J. Li, D. L. Tyrrell, H. Zhang, X.C. Le, CRISPR technology incorporating amplification strategies: molecular assays for nucleic acids, proteins, and small molecules, Chem. Sci. 12 (2021) 4683–4698.
[32] Y.C. Du, S.Y. Wang, Y.X. Wang, J.Y. Ma, D.X. Wang, A.N. Tang, D.M. Kong, Terminal deoxynucleotidyl transferase combined CRISPR-Cas12a amplification strategy for ultrasensitive detection of uracil-DNA glycosylase with zero background, Biosens. Bioelectron. 171 (2021), 112734.
[33] D.X. Wang, J. Wang, Y.C. Du, J.Y. Ma, S.Y. Wang, A.N. Tang, D.M. Kong, CRISPR/Cas12a-based dual amplified biosensing system for sensitive and rapid detection of polynucleotide kinase/phosphatase, Biosens. Bioelectron. 168 (2020), 112556.
[34] H. Yang, C. Wang, E. Xu, W. Wei, Y. Liu, S. Liu, Dual-mode FEN1 activity detection based on Nt.BstNBI-induced tandem signal amplification, Anal. Chem. 93 (2021) 6567–6572.
[35] Y. Dai, R.A. Somoza, L. Wang, J.F. Welter, Y. Li, A.I. Caplan, C.C. Liu, Exploring the trans-cleavage activity of CRISPR-Cas12a (cpf1) for the development of a universal electrochemical biosensor, Angew. Chem., Int. Ed. Engl. 58 (2019) 17399–17405.
[36] M.J. Thompson, V.J.B. Gotham, B. Ciani, J.A. Grasby, A conserved loop-wedge motif moderates reaction site search and recognition by FEN1, Nucleic Acids Res. 46 (2018) 7858–7872.
[37] H.I. Kao, L.A. Henricksen, Y. Liu, R.A. Bambara, Cleavage specificity of *Saccharomyces cerevisiae* flap endonuclease 1 suggests a double-flap structure as the cellular substrate, J. Biol. Chem. 277 (2002) 14379–14389.